www.czasopisma.pan.pl PAN www.journals.pan.pl
Chemical and Process Engineering 2018, 39 (4), 475–489
DOI: 10.24425/cpe.2018.124973

EFFECT OF SONICATION REACTOR GEOMETRY ON CELL DISRUPTION AND PROTEIN RELEASE FROM YEAST CELLS

Jerzy Bałdyga[1]*, Magdalena Jasińska[1], Magdalena Dzięgielewska[2], Monika Żochowska[1]

[1] Warsaw University of Technology, Faculty of Chemical and Process Engineering, ul. Waryńskiego 1, Warsaw, Poland

[2] Industrial Chemistry Research Institute, ul. Rydygiera 8, 01-793 Warsaw, Poland

Dedicated to Professor Andrzej Burghardt on the occasion of his 90th birthday

The measured rate of release of intercellular protein from yeast cells by ultrasonication was applied for evaluating the effects of sonication reactor geometry on cell disruption rate and for validation of the simulation method. Disintegration of two strains of *Saccharomyces cerevisiae* has been investigated experimentally using a batch sonication reactor equipped with a horn type sonicator and an ultrasonic processor operating at the ultrasound frequency of 20 kHz. The results have shown that the rate of release of protein is directly proportional to the frequency of the emitter surface and the square of the amplitude of oscillations and strongly depends on the sonication reactor geometry. The model based on the Helmholtz equation has been used to predict spatial distribution of acoustic pressure in the sonication reactor. Effects of suspension volume, horn tip position, vessel diameter and amplitude of ultrasound waves on the spatial distribution of pressure amplitude have been simulated. A strong correlation between the rate of protein release and the magnitude of acoustic pressure and its spatial distribution has been observed. This shows that modeling of acoustic pressure is useful for optimization of sonication reactor geometry.

Keywords: cell disruption, protein release, *Saccharomyces cerevisiae*, ultrasonication, yeast

1. INTRODUCTION

Yeasts are microscopic, eukaryotic, heterotrophic fungi. The most known and widely used yeast, *Saccharomyces cerevisiae*, is traditionally applied in the production of alcoholic beverages, industrial alcohol and glycerol; it is also used for baking and as an addition to animal feed (Bailey and Ollis, 1986). The cytoplasm of *Saccharomyces cerevisiae* cell is a source of many substances applied in biotechnology, pharmacology, and food industry. Yeast is used for recombinant protein production and as an expression system. Investigations of yeast cells provide insight into genetic, biochemical, and drug discovery research. Yeast cells were intensively investigated, so a complete genomic sequence is available for researchers. They grow rapidly on simple media; amino acids are synthesized from inorganic acids and sulfur containing salts, whereas carbon is often taken from organic media, usually wastes such as molasses, fruit pulps, and milk whey. Moreover, yeasts can grow to high density (Rai and Padh, 2001).

* Corresponding author, e-mail: Jerzy.Baldyga@pw.edu.pl

Yeasts are single cells of 5 to 10 μm size and of spherical or oval shape; they are surrounded by a thick, rigid, enduring cell wall in addition to cell membrane, which makes it difficult to extract the mentioned above desired intracellular products (Zhang et al., 1999). One of the main problems related to yeast utilization and research is thus a choice of a proper method for lysis of cells and extraction of proteins. One can use enzymatic digestion or hydrolysis but they can affect proteins. Another possibility is to use mechanical disruption, applying such processes as bead milling, high pressure treatment or sonication. The most popular is bead milling with glass beads but this method involves harsh conditions, which may result in protein denaturation and decreasing of yield. In this work we consider a method of sonication for cell lysing. This method is usually used to treat small samples; it is fast, efficient and easy to apply (Feliu et al., 1998).

Protein release by ultrasonication of yeast cells has been investigated for many years; more recently it was studied by Liu et al. (2013). They observed effects of acoustic power and duty cycle on degree of cell disruption and the rate of protein release. Ultrasound treatment of yeast, *Aureobasidium pullulans*, was considered by Gao et al. (2014). They observed the effect of initial yeast concentration on survival ratio, namely the survival ratio decreased with a decrease in the initial number of cells. This means that a decrease in the initial cell number increases the relative rate of yeast cell inactivation.

Hohnadel et al. (2014) designed a high-throughput automated external ultrasonic device for rapid lysing of microorganisms including *Saccharomyces cerevisiae* cells. They pointed out that application of specific geometry was the main method to obtain the effective energy transfer between the ultrasonic probe and the sample. The effect of system geometry on the configuration of the ultrasonic field in a sonoreactor was presented by Klima et al. (2007) and Louisnard et al. (2009). By simulation of the acoustic pressure field they showed that production of radicals in the sonoreactor depends on system geometry, for example location of cooling coil. We expect similar effects of sonication system geometry on lysis of yeast cells, and in this sense yeast cells can be treated as model organisms for evaluating mechanical effects of the ultrasonic field, following suggestions of Iida et al. (2008).

Because effects of acoustic power on lysis of yeast cells have been well known for years (Raman et al., 2006), the aim of this study was to investigate experimentally effects of the sonication reactor geometry on lysis of yeast cells and to interpret results based on predicted distributions of the acoustic pressure field. Another objective was to use the measured rates of protein release in systems differing in geometry to evaluate mechanical effects of the ultrasonic field and to validate in this way the model applied to predict the acoustic pressure field.

2. MATERIALS AND METHODS

2.1. Experimental Investigations

Experimental investigations were carried out in the system presented in Fig. 1 using ultrasonic processor operating at an ultrasound frequency of 20 kHz. The system consisted of a glass vessel of diameter D_T and with wall thickness equal to 2 mm that was placed in ice water bath. The effect of vessel diameter was studied using several vessels of diameter between 45 mm and 57 mm. The titanium horn tip of diameter $d_H = 13$ mm was used. Yeast (*Saccharomyces cerevisiae*) suspension in water was ultrasonicated with a Sonics VC 505 supplied by Sonics (500 W maximum power). Sonics VC 505 allows ultrasonic vibrations at the probe tip to be set to any desired amplitude and ensures uniform probe amplitude regardless of the varying loading conditions. In present investigations five values of the emitter amplitude, A, were used: 24.8 μm, 49.6 μm, 74.4 μm, 99.2 μm and 124.0 μm.

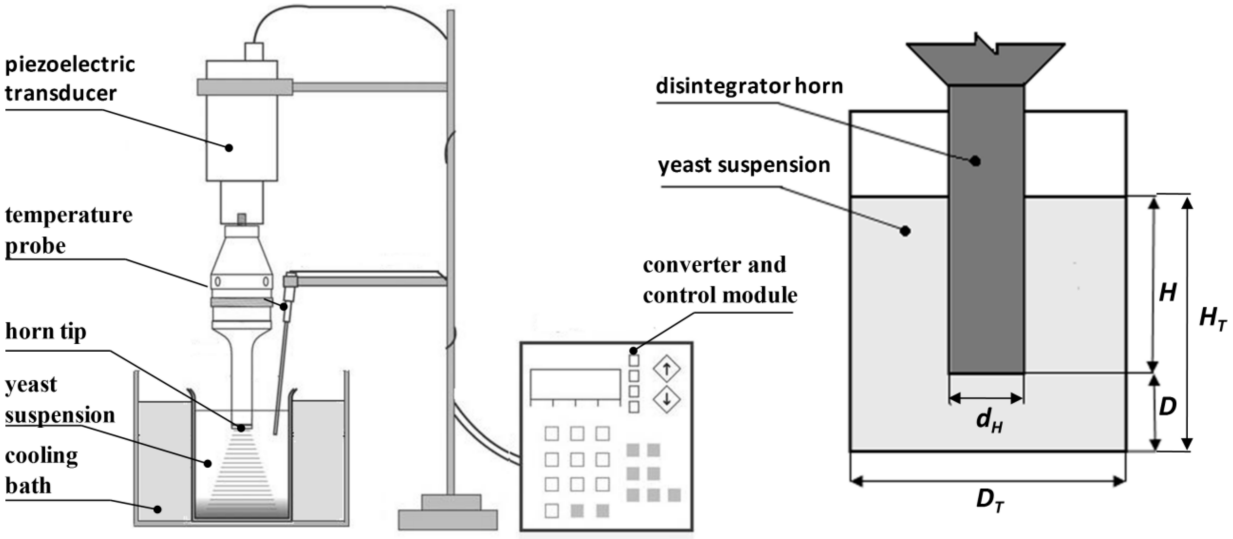

Fig. 1. Schematic of the experimental set-up and geometry of the sonication vessel

Two strains of *Saccharomyces cerevisiae* were applied, to compare kinetics of protein release observed for different strains. Strain 1 was from Lesaffre, Wołczyn, Poland, strain 2 was from Lallemand, Lublin, Poland. Both of them are widely-used commercial baking strains of wild type. Nucleic acid and protein sequences of *S. cerevisiae* RedStar strain one can find in www.yeastgenome.org. Lallemand is known as one of pregenitor strains of S288C, X2180-1A and X2180-1B. The dry mass of *Saccharomyces cerevisiae* was measured before each sonication experiment after 2 hours of drying in 105 °C. Based on twelve measurements in each case, the average values of dry mass were identifies as equal to 31.3 w/w% and 30.6 w/w% for strains 1 and 2 respectively; related values of the variation coefficient were 0.70% and 0.86%. The yeast suspension applied for disintegration experiments was containing 0.31 g of dry mass per 100 cm^3 of suspension. The disintegration process was carried out at 20 ± 3 °C.

The sonication was carried out in the intermittent mode; the on/off pulser was applied, and on and off cycles, both equal to 5 seconds, were controlled independently. In most experiments the complete process time (including on and off periods) was equal to 180 s; longer sonication time was applied in experiments performed to identify kinetics of protein release. This, together with placing the vessel in the ice water bath, enabled to control the temperature; when starting experiment at 20 °C the final temperature in the vessel was never smaller than 19.7 °C and never exceeded 20.3 °C.

The influence of process conditions on efficiency of ultrasonic disruption was investigated by measuring the amount of released soluble protein. The yeast suspension was centrifuged (MPW 223e) and the supernatant liquid containing dissolved proteins was collected and diluted ten-fold before measuring concentration. Concentration of proteins released to the aqueous phase from the disintegrated yeast cells was measured using the Lowry method (Lowry et al., 1951). The Lowry method is based on two complexing reactions. The first one is the copper complexing of amino acids constituting proteins in an alkaline medium. In the second reaction the Folin reagent reacts with the aromatic amino acids of the proteins. The absorbance of formed complexes is determined spectrophotometrically; in this work Hitachi U-1900 and Spectronic 601 by Milton Roy spectrophotometers were used at a wave length of 750 nm. A standard curve was constructed using protein solution BSA A9647-10G. As the absorbance readings for samples were falling within the linear portion of the standard curve, the total protein concentrations S of the samples were estimated using the linear regression method, yielding $S = 338.2 \cdot A_\lambda$, with the coefficient of determination, R^2; $R^2 = 0.987$, where A_λ represents the net absorbance obtained by subtracting the background measurements from protein measurements.

2.2. Modeling of Acoustic Pressure Field

In the sonication process the yeast cell walls are disrupted and thus the cells are disintegrated by very high shear forces that are induced by the collapsing cavitation bubbles. The ultrasonic field propagates in the liquid medium from the emitter surface by pressure waves that periodically expand and compress the medium, which can create locally the above mentioned transient cavitation microbubbles. As mentioned earlier the acoustic pressure distribution depends on the system geometry, medium and sonication vessel properties, and sonication power.

For homogeneous media one can assume the linear wave propagation, which leads to the wave equation that describes distribution in space and variation in time of an acoustic pressure.

$$\nabla^2 p - \frac{1}{c^2}\frac{\partial^2 p}{\partial t^2} = 0 \tag{1}$$

One should remember that Eq. (1) is valid under the assumption that the effects of viscosity and thermal conductivity of the fluid are negligible. This is possible when the viscous relaxation time

$$\tau_\nu = \frac{4}{3}\frac{\nu}{c^2} \tag{2}$$

and the thermal relaxation time

$$\tau_\kappa = \frac{\kappa}{c^2} \tag{3}$$

that are defined based on the fluid kinematic viscosity, ν, and the fluid thermal diffusivity κ, are small enough to fulfil the conditions $\omega\tau_\nu \ll 1$ and $\omega\tau_\kappa \ll 1$. This is true for pure water when the ultrasound frequency is equal to 20 kHz.

Assuming that the acoustic pressure is time harmonic, so can be expressed by $p(\vec{r},t) = P(\vec{r})\cdot e^{i\omega t}$, one can transform Eq. (1) to the Helmholtz equation

$$\nabla^2 P(\vec{r}) + \frac{\omega^2}{c^2}P(\vec{r}) = \nabla^2 P(\vec{r}) + k^2 P(\vec{r}) = 0 \tag{4}$$

with ω being an angular frequency, and k representing the wave number, $k = \omega/c$. By solving Equation (4) with adequate boundary conditions we get the spatial distribution of pressure amplitude, $P(\vec{r})$. The instantaneous pressure can be then calculated from the field of the pressure amplitude, $P(\vec{r})$, using Equation (5):

$$p(\vec{r},t) = \Re[P(\vec{r})]\cos(\omega t) - \Im[P(\vec{r})]\sin(\omega t) \tag{5}$$

In the case of one-dimensional system, there is an analytical solution of Eqs. (1), (4), (5) with the boundary condition $P(0) = P_A$ for propagation of plane acoustic waves in direction x from the emitter surface placed at $x = 0$:

$$p(x,t) = P_A[\cos(\omega t)\cos(-kx) - \sin(\omega t)\sin(-kx)] = P_A\cos(\omega t - kx) \tag{6}$$

with $k = \omega/c$, which shows not damped oscillations. When in the liquid there are suspended yeast cells as well as air or vapor bubbles generated by cavitation then the acoustic waves can be highly attenuated. In the case of linear mono-harmonic wave, attenuation effect can be represented by a complex wave number (Temkin, 2005).

$$k = k_R - i\alpha \tag{7}$$

After introducing this to Eq. (4) and considering again propagation of plane acoustic waves in direction x one gets instead of Eq. (6)

$$p(x,t) = P_A e^{-\alpha x}\cos(\omega t - kx) \tag{8}$$

which shows that amplitude of the waves decays as $\exp(-\alpha x)$.

In the case of solving Eq. (4) for the experimental system the problem becomes much more complex, so we apply some simplifying assumptions similar to those used by Klima et al. (2007) and Raman et al. (2006). The simplifications are related to application of ideal boundary conditions. The boundary conditions applied to solve Eq. (4) for the system presented in Figure 1 are as follows: an infinitely soft boundary at water-air interface is assumed, so $P(\vec{r}) = 0$ there, the pressure amplitude at the emitter surface is denoted byP_A, so $P = P_A$ there, and the other walls are assumed to be infinitely rigid, so one has $\partial P/\partial n = 0$ at the walls. To perform simulations with these ideal boundary conditions one needs to specify the pressure amplitude at the emitter surface; this value has been calculated from Eq. (9) based on "plane traveling wave approximation" for chosen process parameters.

$$P_A = \rho_L A \omega c = \sqrt{2\rho_L c I_s} \tag{9}$$

where A is the emitter amplitude and I_s represents the ultrasonic intensity at the emitter surface that is defined as the power transmitted to the sonication vessel per unit area of the emitter surface. The boundary conditions are presented in Figure 2 for the system geometry shown in Fig. 1.

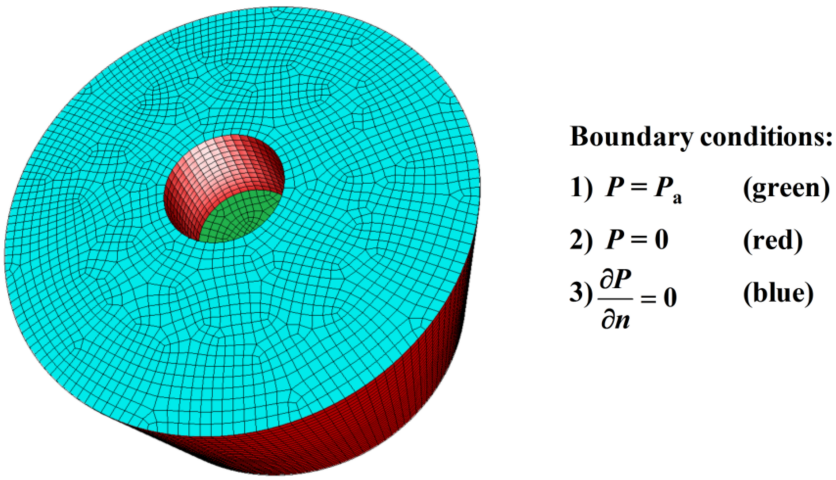

Fig. 2. Boundary conditions applied in simulations

It should be noted that due to idealized boundary conditions the results should be treated as an approximation; a more complex approach involving vibration of the boundaries one can find in Louisnard et al. (2009). In Tudela et al. (2014) one can find a review of modeling the spatial distribution of the acoustic pressure including limitations of currently applied methods and upcoming modeling challenges.

Application of ideal boundary conditions has consequences for process interpretation. Effect of vibrating vessel walls on suspended cells cannot be considered. Also the difference between nucleation of cavitation bubbles in wall nucleation sites and bubble nucleation in the bulk is not considered; we just compare predicted distributions of pressure amplitude to show possible effects of the sonication reactor geometry on the process.

Computations presented in this work have been performed using the free software Elmer 6.0. The mesh was generated using Gambit software. A structured numerical grid consisted of about 65,000 hexahedral computational cells. It has been checked that the results of computations were not sensitive to a further increase of the number of cells. Results of computations are presented as the spatial distributions of the pressure amplitude, $P(\vec{r})$, within the sonication vessel, and they are confronted with experimental data for cell dispersion.

3. RESULTS OF EXPERIMENTAL INVESTIGATIONS

Results of experiments are presented in what follows. Effects of the horn tip position, D, and its amplitude, A, on the protein release are shown in Figure 3 for strain 1 of *Saccharomyces cerevisiae*. Figure 4 shows effects of the horn tip position, D, and the diameter of the sonication vessel, D_T, on protein release. Both figures show the minimum point on a curve representing the concentration of protein released after fixed time of 180 s versus the distance between the vessel bottom and the emitter surface. The protein release increases with increasing the emitter amplitude (Figure 3); it also increases with increasing sonication vessel diameter at constant suspension volume (Figure 4). Both observations are further confirmed by experimental data presented in Figs. 5 and 6. Figures 5 and 6 show high sensitivity of protein concentration to the emitter amplitude; Fig. 5 confirms additionally effect of sonication vessel diameter observed in Fig. 4; there is indeed a gentle, monotonic increase of protein concentration with increasing vessel diameter.

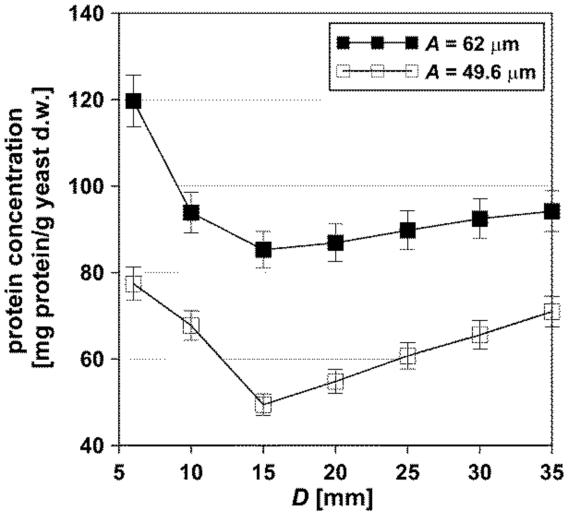

Fig. 3. Effect of horn tip position, D, and its amplitude on protein concentration; $V = 75$ cm^3, $D_T = 48$ mm, $d_H = 13$ mm, $f = 20$ kHz, process time = 180 s, strain 1 of *Saccharomyces cerevisiae*

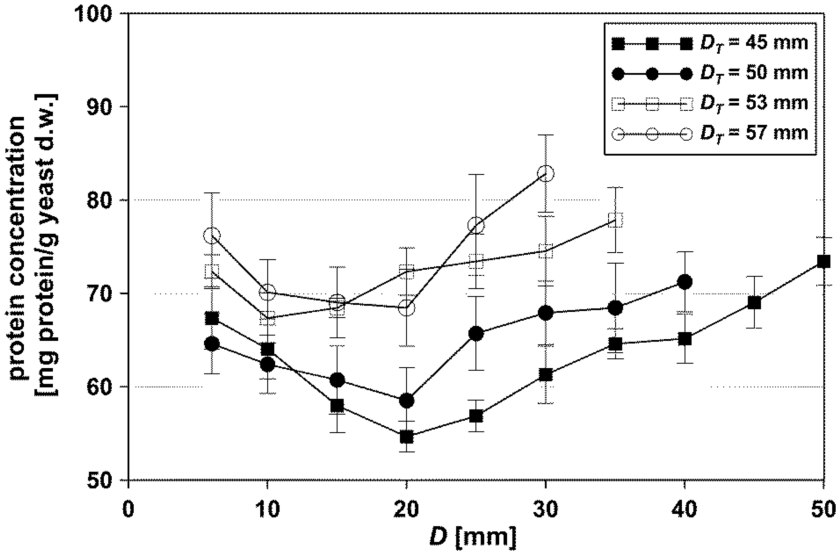

Fig. 4. Effect of horn tip position, D, and sonication vessel diameter, D_T, on protein concentration; $V = 90$ cm^3, $d_H = 13$ mm, $f = 20$ kHz, $A = 62$ μm, process time = 180 s, strain 2 of *S. cerevisiae*

Effect of the suspension volume on the protein release for two strains of *Saccharomyces cerevisiae* is presented in Fig. 7. A monotonic decrease of the concentration of released protein with increasing the sample volume is observed in both cases, and the strain number 1 is slightly more sensitive to the volume variation than the strain number 2. A measured variation with time of the released protein concentration is presented and interpreted in Section 4 of this paper.

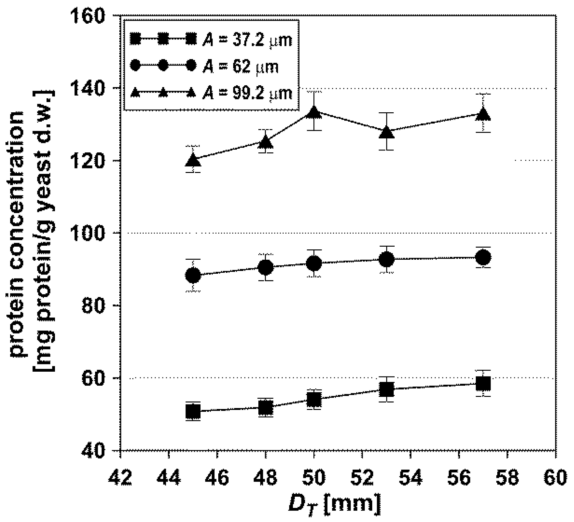

Fig. 5. Effects of sonication vessel diameter, D_T, and amplitude of emitter surface, A, on protein concentration; $V = 70$ cm^3, $d_H = 13$ mm, $f = 20$ kHz, $D = 15$ mm, process time = 180 s, strain 2 of *S. cerevisiae*

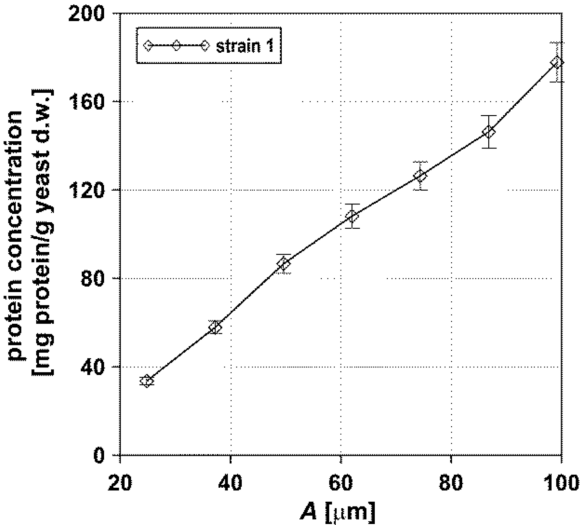

Fig. 6. Effect of amplitude of emitter surface, A, on protein concentration; $V = 50$ cm^3, $d_H = 13$ mm, $f = 20$ kHz, $D = 15$ mm, process time = 180 s, strain 1 of *S. cerevisiae*

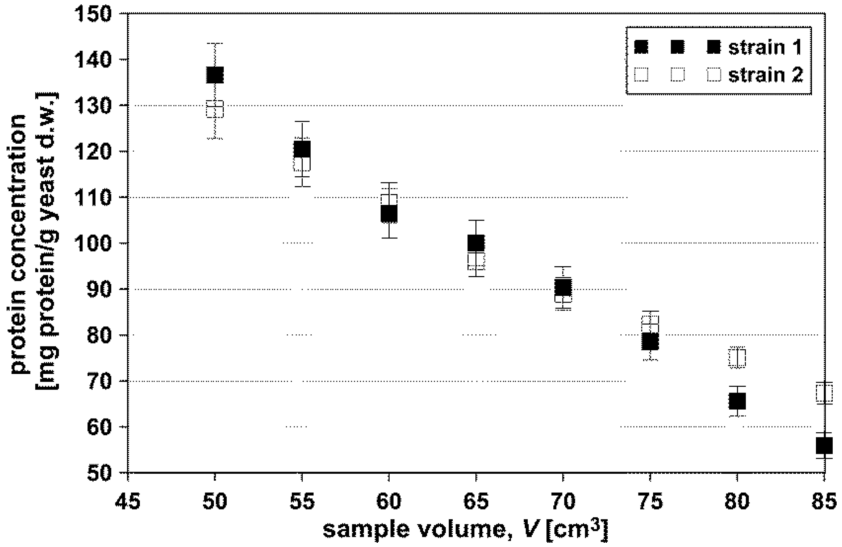

Fig. 7. Effect of the suspension volume on protein concentration for two strains of *Saccharomyces cerevisiae*; $D_T = 48$ mm, $D = 15$ mm, $d_H = 13$ mm, $f = 20$ kHz, $A = 62$ μm, process time = 180 s

Average values and standard deviations shown in Figs. 3 to 7 are based on averaging of several measurements of concentration after experiment; the time variation of concentration presented in the Section 4 is based on a single measurement for each point.

4. RESULTS OF MODELING AND INTERPRETATION OF EXPERIMENTAL DATA

We start from investigation of the effect on propagation of ultrasonic waves of the distance from the vessel bottom, D, to emitter surface. Results of simulations presented in Fig. 8 agree qualitatively with observations of Klima et al. (2007). Instead of the spatial distribution of the pressure amplitude Klima et al. (2007) presented distribution of the ultrasonic intensity, $I(\vec{r})$, that is defined by analogy to properties of plain traveling waves

$$I(\vec{r}) = \frac{P(\vec{r})^2}{2\rho_L c} \tag{10}$$

Klima et al. (2007) observed that the decrease in $I(\vec{r})$ when increasing the distance from the emitter surface to the vessel bottom can be reversed to the intensity increase due to multiple reflections by increasing the distance D.

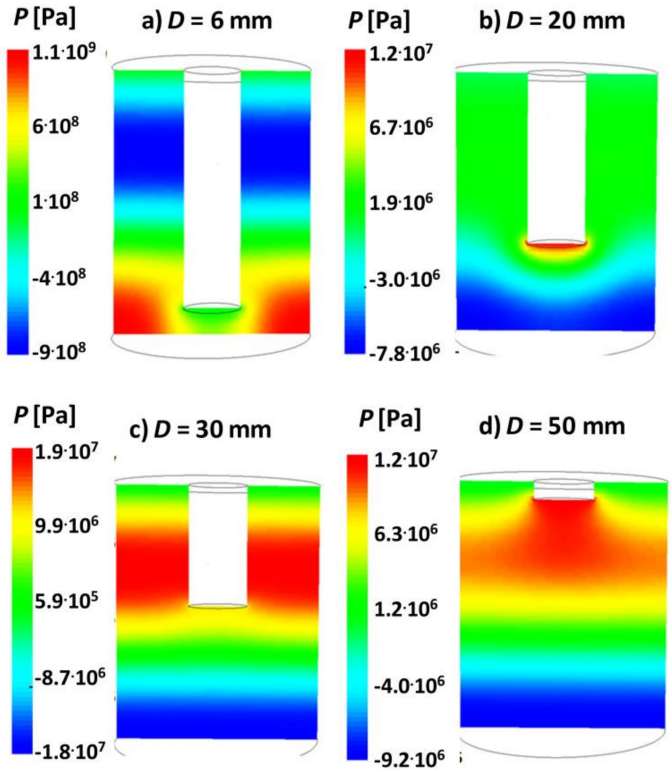

Fig. 8. Effect of the distance from the vessel bottom to emitter surface, D, on spatial distribution of pressure amplitude, P [Pa]; $V = 90$ cm^3, $D_T = 45$ mm, $d_H = 13$ mm, $f = 20$ kHz, $A = 62$ μm

Figure 8 shows a decrease in the pressure amplitude when increasing the distance from the emitter surface to the vessel bottom from 6 to 20 mm and an increase in the amplitude when the distance D increases from 20 mm to 30 mm and 50 mm.

Results of simulations agree with experimental results: comparison of Fig. 8 with Figs. 3 and 4 shows that the variation in ultrasonic intensity observed when increasing the distance from the emitter surface to the vessel bottom, D, results in similar efficiency of protein release. Minimum acoustic pressure for D close to 20 mm observed for $D_T = 50$ mm results in minimum release of protein for D in a range between 15 mm and 20 mm.

Effects of vessel diameter, D_T, and vessel volume, V, on distribution of acoustic pressure are presented in Figs. 9 and 10, respectively.

Predicted effect of sonication vessel diameter (Fig. 9) agrees well with the results of experimental investigations presented in Fig. 4. Simulation results of the effect of increase of the suspension volume that are presented in Figure 10 show relative decrease of the volume active for cell disruption. This phenomenon is well observed in Fig. 7, where monotonic decrease of protein concentration with increasing suspension volume is observed.

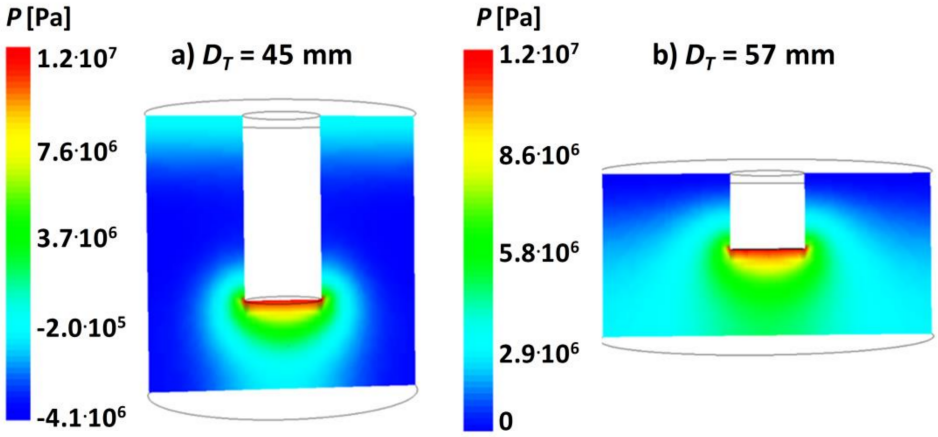

Fig. 9. Effect of the sonication vessel diameter on spatial distribution of pressure amplitude, P [Pa]; $V = 70$ cm^3, $D = 15$ mm, $d_H = 13$ mm, $f = 20$ kHz, $A = 62$ μm

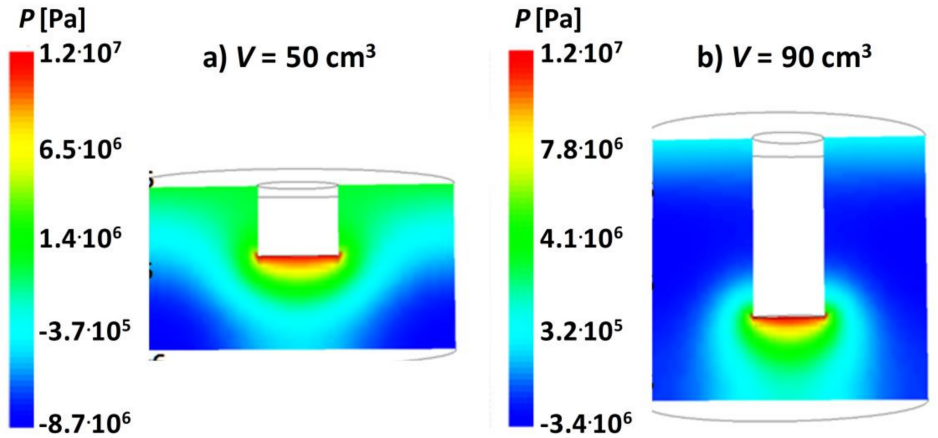

Fig. 10. Effect of the sonication vessel volume on spatial distribution of pressure amplitude, P [Pa]; $D_T = 50$ mm, $D = 15$ mm, $d_H = 13$ mm, $f = 20$ kHz, $A = 62$ μm

Also effects of oscillation amplitude of the emitter surface were simulated. Results of simulations show similar distributions of the acoustic pressure for different values of the amplitude, with the smallest and the largest pressure both proportional to the amplitude at the emitter surface. For example for $A = 24.8$ μm the smallest and the largest pressure values were equal to -2.8 MPa and 4.60 MPa, for $A = 62$ μm, -5.2 MPa and 11.5 MPa,for $A = 124$ μm, -10.4 MPa and 23.0 MPa respectively. This proportionality results from application of the linear model for sound wave propagation for a given geometrical configuration.

The presence of bubbles and yeast cells complicates this simple interpretation. As discussed earlier attenuation of acoustic waves results from dissipative phenomena caused by liquid viscosity, presence of cavitation bubbles and presence of yeast cells. In the case of linear, mono-harmonic waves attenuation effect can be expressed using the attenuation coefficient, α, that is then used to define a complex wave number $k = k_R - i\alpha$. The wave number $k = k_R - i\alpha$ has to be then substituted into Eq. (4). To show sensitivity of simulation results to the attenuation coefficient let us consider a bubbly liquid composed of air

bubbles of diameter 100 μm dispersed in water. Using the method proposed by Temkin (2005), presented in chapter 9.4 of his book, we estimate for the bubble volume fraction equal to 10^{-7} the attenuation coefficient $\alpha = 0.01$ m^{-1} and the phase velocity equal to sound speed, c, whereas for the bubble volume fraction equal to 10^{-2} the attenuation coefficient $\alpha = 450$ m^{-1} and the phase velocity equal to about $0.07c$.

Results of simulations presented in Fig. 11 show that despite huge increase of attenuation coefficient due to presence of bubbles, resulting pressure distributions have a similar shape and a similar range of variation, just the region of high ultrasonic intensity is smaller in the case of $\alpha = 450$ m^{-1}, which means that effect of bubble presence does not change our conclusions. Also increase of cell concentration increases the attenuation coefficient, which explains effect of initial yeast concentration on yeast cell inactivation observed by Gao et al. (2014).

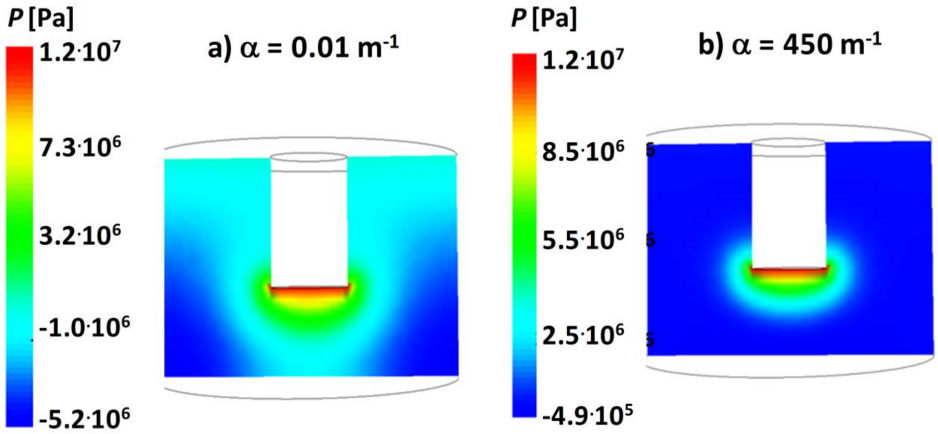

Fig. 11. Effect of dumping by cavitation bubbles on spatial distribution of pressure amplitude, P [Pa]; $V = 70$ cm^3, $D_T = 50$ mm, $D = 15$ mm, $d_H = 13$ mm, $f = 20$ kHz, $A = 62$ μm: a) bubble volume fraction equal to 10^{-7}, b) bubble volume fraction equal to 10^{-2}

Presented results of comparison of model predictions with experimental data support the method proposed by Iida et al. (2008), which is based on the assumption that the release rate of intercellular protein from yeast cells by the ultrasonic action can be used for evaluating the physical (mechanical) effects of the ultrasonic field.

Release of protein in time can be interpreted as the first order kinetics process and described using classical relation reported by Doulah (1977)

$$C = C_{\max} \cdot [1 - \exp(-Kt)] \tag{11}$$

where K represents the protein release constant and C denotes the concentration of released proteim per gram of dry mass. The maximum protein release represnts the asymptotic values of C measured after long time:

- for strain 1: $C_{\max} = 297.0 \pm 1.6$ mg protein/g yeast d.w.
- for strain 2: $C_{\max} = 349.6 \pm 4.4$ mg protein/g yeast d.w.

The ratio $C/C_{\max}$ is referred to as the protein release. To identify the values of the protein release constant, K, using the least squares method, Eq. (11) has been transformed to $\ln\left[(1 - C/C_{\max})^{-1}\right] = Kt$. The values of determination coefficient, R^2 are rather high, between $R^2 = 0.952$ for $A = 24.8$ μm and $R^2 = 0.991$ for $A = 124.0$ μm. Figure 12 shows some differences in time variation of protein concentration in both considered strains. However, in both cases the form of Eq. (11) agrees with experimental data, which enables identification of the protein release constant.

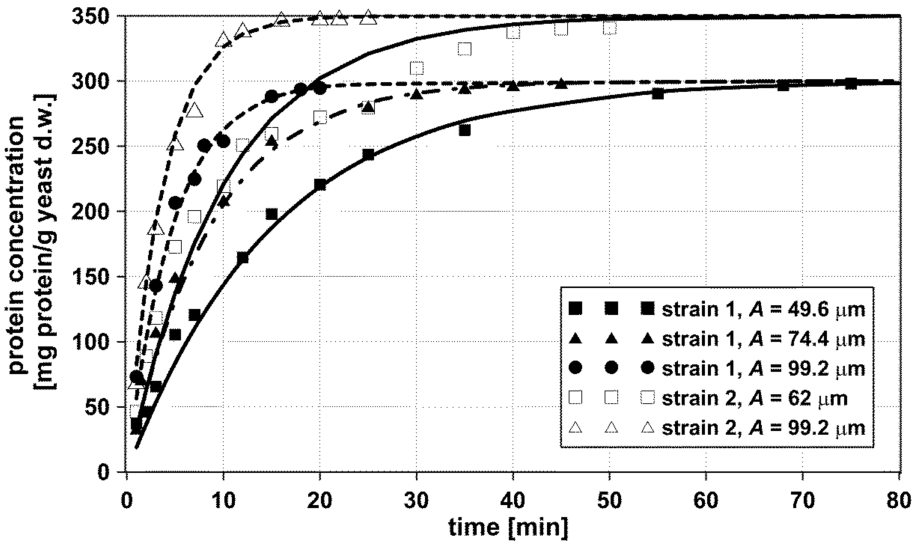

Fig. 12. Protein release versus time: effect of amplitude of emitter surface, A, on protein concentration for two strains of *Saccharomyces cerevisiae* $V = 50$ cm^3, $D_T = 50$ mm, $D = 15$ mm, $d_H = 13$ mm, $f = 20$ kHz; periodic operation: 5 s on, 5 s off

Dependence of the protein release constant on the amplitude of oscillations of the emitter surface, A, is presented in Fig. 13. One can see that the constant K is roughly proportional to A^2. In fact as shown by Doulah (1977) one can expect

$$K \propto (P_a - P_{a_0})^{\beta} \tag{12}$$

where P_a is the power input and P_{a0} represents the cavitation threshold power, i.e. the smallest power for which in the investigated system cavitation is observed that is able to cause protein release. Iida et al., (2008) estimated the threshold value for the protein release equal to about 5 W. An exponent β was introduced by Doulah (1976) to account for mechanism of cell disruption; more precisely it is related to the ratio of the cell size to the size of the violent eddies causing cell disruption. From presented results we get $\beta \approx 1 (pm 0.05)$, which agrees with results for *Acetobacter peroxydans* (Kapucua et al., 2000) and *E. Coli*, (Garcia et al., 2015) whereas Doulah (1977) reports $\beta \approx 0.9$ for yeast cells. A much smaller

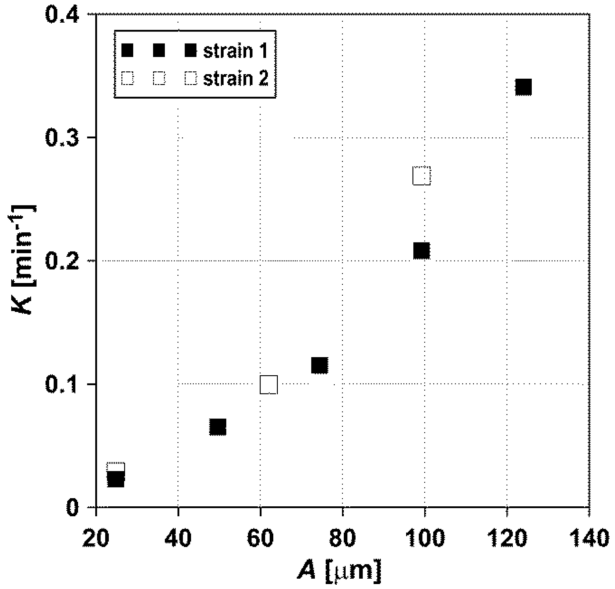

Fig. 13. Protein release constant versus amplitude of emitter surface, A, for two strains of *Saccharomyces cerevisiae* $V = 50$ cm^3, $D_T = 50$ mm, $D = 15$ mm, $d_H = 13$ mm, $f = 20$ kHz; periodic operation: 5 s on, 5 s off

value of this constant, namely 0.3558, was obtained by Liu et al. (2013). This may result from the fact that they did not use in their kinetics the cavitation threshold power, P_{a0}. Garcia et al. (2015) investigated hemoglobine release kinetics and observed $\beta \approx 1.16$.

Character of dependence of the protein release constant K on the amplitude of the emitter surface oscillations and almost identical values of K observed for different strains shown in Fig. 13 can be explained by substituting for the power, P_a (Bałdyga et al., 2008)

$$P_a = \frac{1}{2} S_e \rho_L c (\omega A)^2 \tag{13}$$

where S_e represents the surface of emitter. Then, for $\beta = 1$, Eq. (12) takes the form

$$K = C_x S_e \rho_L c \, \omega^2 (A - A_0)^2 \tag{14}$$

In the present case estimated from Eq. (14) value of A_0 is close to zero, $A_0 = 0.012$ μm. Notice that whereas maximum release from both considered strains is different (300 and 350 mg/g yeast d.w. as shown in Fig. 12), the protein release constant takes very similar values. This results from the fact that for a given geometry the protein release constant expressed by Eq. (14) depends on the mechanical parameters, angular frequency ω and the emitter amplitude A.

Using the maps of the pressure amplitude as presented in Figs. 8 to 11 one can identify the region of cavitation and characterize related stresses. Stresses generated by cavitation in the case of ultrasonic devices are much larger than hydrodynamic stresses generated by the flow and the velocity difference between oscillating fluid and oscillating cells (Bałdyga et al., 2008). Cavitation occurs when the pressure falls sufficiently low, which can be characterized by the cavitation number:

$$CN = \frac{p - p_V(T)}{\frac{1}{2}\rho_L U_\infty^2} \tag{15}$$

Cavitation occurs when CN is reduced below a limiting value called incipient cavitation number.

The stresses resulting from cavitation can be calculated from Eq. (16) proposed by Crum (1988).

$$\tau_c = \alpha' \rho_L c \, u_j \tag{16}$$

where α' is a constant between 0.41 and 3.0, and u_j represents the microjet velocity

$$u_j = \frac{(p - p_V)}{0.915 \rho_L^{1/2}} \tag{17}$$

Both an extent of the cavitation zone as well as cavitation stresses expressed by Eqs. (16) and (17) depend on the distribution of the pressure amplitude, P. For the emitter amplitude A changing from 24.8 μm to 124.0 μm the maximum stresses predicted from Eq. (16) increase from 110 MPa to 240 MPa. They are for the whole range of A higher than the mean maximum von Mises stress-at-failure $\sigma_{VM} = 70 \pm 4$ MPa as determined by Smith et al. (2000), so in each case release of protein is possible in some regions of the sonication vessel. A threshold amplitude P to observe stresses higher than 70 MPa can be predicted from Eqs. (16) and (17) to be about $5 \cdot 10^5 - 10^6$ Pa. However, intensity of cavitation and intensity of protein release increase with increasing the pressure amplitude P. Figures 8 to 11 show very clearly that the value and distribution of amplitude P depend both on the system geometry and the value of emitter amplitude with described above consequences for protein release.

5. CONCLUSIONS

One can conclude that the modeling based on the Helmholtz equation, even when simplified approach is used that neglects effects of attenuation and employs idealized boundary conditions, can be very helpful for identification of optimal process conditions for protein release from yeast cells. This is very well observed when geometry of the sonication vessels varies. We have found that especially position of ultrasonic horn and suspension volume affect significantly protein release. In any case there is a very good qualitative agreement between model predictions and experimental data.

Predicted sensitivity of simulation results to the attenuation coefficient resulting from presence of bubbles or cells shows that resulting pressure distributions, at least in present computations, have a similar shape and a similar range of variation, but the region of high ultrasonic intensity decreases. This means that effect of bubbles or cells does not change the general conclusion that this kind of modeling can be useful for process development.

Presented results of comparison of model predictions with experimental data support the assumption of Iida et al. (2008) that the release rate of intercellular protein from yeast cells by the ultrasonic action can be used for evaluating the mechanical effects of the ultrasonic field. More precisely it has been shown in this paper that experimental data showing effects of process conditions on protein release can be interpreted using the concept of protein release constant. Dependence of this kinetic constant on the emitter amplitude and frequency agrees very well with presented theoretical interpretations. The values of the protein release constant are very similar for both considered yeast strains of different origin, due to the fact that the protein release constant K depends mainly on mechanical parameters. The cavitation threshold amplitude, A_0, the only parameter in the model which can depend on cell properties is in present case very small. This shows that rather mechanical phenomena than details of yeast cell structure or composition of solution control in the considered case the process of protein release.

The authors acknowledge the financial support from Polish National Science Centre (Grant agreement number: UMO-2017/27/B/ST8/01323).
Part of this work was financially supported by Warsaw University of Technology.

SYMBOLS

A	emitter amplitude, m
A_0	cavitation threshold amplitude for considered emitter and considered cells, m
A_λ	net absorbance
C	concentration of released protein per gram of dry mass, g/kg
C_x	constant of proportionality in Equation (14)
CN	cavitation number
c	speed of sound, m/s
D	horn tip position, m
D_T	vessel diameter, m
d_h	horn tip diameter, m
f	frequency, kHz
H	distance of the horn tip from the liquid level, m
H_T	liquid level, m
I_s	ultrasonic intensity, W/m^2

K protein release constant, s^{-1}
k wave number, m^{-1}
P pressure amplitude, Pa
P_A pressure amplitude at the emitter surface, Pa
P_a power input, W/kg
P_{a0} cavitation threshold power, W/kg
p acoustic pressure, Pa
p_V saturated vapour pressure
$\vec{r}$ position vector, m
S total protein concentration, μg/mL
S_e surface of emitter, m^2
t time, s
U_∞ reference velocity, m/s
u_j jet velocity
V suspension volume, m^3
x position in one-dimensional system, m

Greek letters

α attenuation coefficient, m^{-1}
β exponent in Eq. (12)
κ thermal diffusivity, m^2/s
ν kinematic viscosity, m^2/s
ρ_L fluid density, kg/m^3
σ_{VM} von Mises stress-at-failure, Pa
τ_c cavitation stress, Pa
τ_k thermal relaxation time, s
τ_ν viscous relaxation time, s
ω angular frequency, s^{-1}

REFERENCES

Bailey J.E., Ollis D.F., 1986. *Biochemical engineering fundamentals*. McGraw-Hill Book Company, New York.

Bałdyga J., Makowski Ł., Orciuch W., Sauter C., Schuchmann H.P., 2008. Deagglomeration processes in high-shear devices. *Chem. Eng. Res. Des.*, 86, 1369–1381. DOI: 10.1016/j.cherd.2008.08.016.

Crum L., 1988. Cavitation microjets as a contributory mechanism for renal disintegration. *ESWL. J. Urol.*, 148, 1587–1590. DOI: 10.1016/S0022-5347(17)42132-X.

Doulah M.S., 1977. Mechanism of disintegration of biological cells in ultrasonic cavitation. *Biotechnol. Bioeng.*, 19, 649–660. DOI: 10.1002/bit.260190504.

Elmer 6.0, http://www.csc.fi/elmer.

Feliu J.X., Cubarsi R., Villaverde A., 1998. Optimized release of recombinant proteins by ultrasonication of *E. coli* cells. *Biotechnol. Bioeng.*, 58, 536–540. DOI: 10.1002/(SICI)1097-0290(19980605)58:5<536::AID-BIT10>3.0.CO;2-9.

Gao S., Hemar Y., Ashokkumar M., Paturel S., Gillian D. Lewis G. D., 2014. Inactivation of bacteria and yeast using high-frequency ultrasound treatment. *Water Res.*, 60, 93–104. DOI: 10.1016/j.watres.2014.04.038.

Garcia R.A., Clevenstine S.M, Piazza G.J., 2015. Ultrasonic processing for recovery of chicken erythrocyte hemoglobin. *Food Bioprod. Process.*, 94, 1–9. DOI: 10.1016/j.fbp.2014.12.002.

Hohnadel, M., Felden, L., Fijuljanin D., Jouette, S., Chollet, R., 2014. A new ultrasonic high-throughput instrument for rapid DNA release from microorganisms. *J. Microbiol. Methods*, 99, 71–80. DOI: 10.1016/j.mimet.2014.02.004.

Iida Y., Tuziuti T., Yasui K., Kozuks T., Towata A., 2008. Protein release from yeast cells as an evaluation method of physical effects in ultrasonic field. *Ultrason. Sonochem.*, 15, 995–1000. DOI: 10.1016/j.ultsonch.2008.02.013.

Kapucua H., Gulsoy N., Mehmetoglu U., 2000. Disruption and protein release kinetics by ultrasonication of *Acetobacter peroxydans* cells. *Biochem. Eng. J.*, 5, 57–62. DOI: 10.1016/S1369-703X(99)00065-0.

Klima J., Frias-Ferrer A., Gonzales-Garcia J., Ludvik J., Saez V., Iniesta J., 2007. Optimization of 20 kHz sonoreactor geometry on the basis of numerical simulation of local ultrasonic intensity and qualitative comparison with experimental results. *Ultrason. Sonochem.*, 16, 250–259. DOI: 10.1016/j.ultsonch.2006.01.001.

Liu D., Zeng X.-A, Da-Wen Sun D.W., Han Z., 2013. Disruption and protein release by ultrasonication of yeast cells. *Innovative Food Sci. Emerg. Technol.*, 18, 132–137. DOI: 10.1016/j.ifset.2013.02.006.

Louisnard O., Gonzales-Garcia J., Tudela I., Klima J., Saez V., Vargas-Hernandez Y., 2009. FEM simulation of a sono-reactor accounting for vibration of the boundaries. *Ultrason. Sonochem.*, 14, 19–28. DOI: 10.1016/j.ultsonch.2008.07.008.

Lowry O.H., Rosebrough N.J., Farr A.L, Randall R.J., 1951. Protein measurement with the folin phenol reagent. *J. Biol. Chem*., 193, 265–275.

Rai M., Padh H., 2001. Expression systems for production of heterologous proteins. *Current Science*, 80(9), 1121–1128.

Raman V., Abbas A., Joshi S.C., 2006. Mapping local cavitation events in high intensity ultrasound fields. *Proceeding of the COMSOL Users Conference*. Bangalore, 2006, 1–6.

Smith A.E., Moxham K.E., Middelberg A.P.J., 2000. Wall material properties of yeast cells. Part II. Analysis. *Chem. Eng. Sci.*, 55, 2043–2053. DOI: 10.1016/S0009-2509(99)00501-1.

Temkin S., 2005. *Suspension acoustics*. Cambridge University Press. DOI: 10.1017/CBO9780511546129.001.

Tudela I., Saez V., Esclapez M. D., Diez-Garcia M. I., Bonete P., Gonzales-Garcia J., 2014. Simulation of the spatial distribution of the acoustic pressure in sonochemical reactors with numerical methods: A review. *Ultrason. Sonochem.*, 21, 909–919. DOI: 10.1016/j.ultsonch.2013.11.012.

Zhang N., Gardner D.C., Oliver S.G., Stateva L.I., 1999. Genetically controlled cell lysis in the yeast *Saccharomyces cerevisiae*. *Biotechnol. Bioeng.*, 64, 607–615. DOI: 10.1002/(SICI)1097-0290(19990905)64:5<607::AID-BIT11>3.0.CO;2-0.

Received 26 July 2018
Received in revised form 15 October 2018
Accepted 23 October 2018